

# Learning distant paths with traveling waves

<sup>1</sup>Yoshiki Ito    <sup>2,3</sup>Taro Toyozumi

November 2019

## Abstract

Traveling waves are commonly observed across the brain. While previous studies have suggested the role of traveling waves in learning, the mechanism is still unclear. We adopted a computational approach to investigate the effect of traveling waves on synaptic plasticity. Our results indicate that traveling waves facilitate learning of distant and indirectly connected network-paths when combined with a reward-based local synaptic plasticity rule. We demonstrate that traveling waves expedite finding the shortest paths and learning nonlinear input/output-mapping, such as the XOR function.

## 1, Introduction

Waves of neural activity in the brain play an essential role in our recognition and learning (Klimesch, 1996). Among them, traveling waves are observed at different spatial scales in many brain regions by different recording methods, such as electroencephalogram (EEG) (Burkitt et al., (2000); Nunez and Srinivasan, (2006); Srinivasan et al., (2006a)), voltage-sensitive dyes (VSD) (Grinvald et al., (1994); Slovins et al. (2002)), and local field potential (LFP) (Nauhaus et al., (2009); Nauhaus et al. (2012)). Traveling wave is typically observed in mild anesthesia (Mohajerani et al., (2010); Nauhaus et al., (2009)), sleep (Massimini et al., (2004)), or idle (Sakata and Harris, (2009)).

Cortical traveling waves consist of the upstate and downstate of neurons and propagate these phases in coherence. (Harris and Thiele (2011); Petersen et al., (2003); Steriade et al., (1993); Krull et al., (2019)) The upstate is defined by relatively large membrane potential fluctuations with a high firing rate, while the downstate is referred to as a phase of small fluctuations with little spikes (Lee et al. (2008)). The propagation of this up/down state is estimated to be slower than the axonal signal transmission, and the activity spreads both as subthreshold and suprathreshold responses. (Sato et

---

1, Graduate School of Information and Technology, the Department of Mechano-Informatics, University of Tokyo, Tokyo, Japan

2, Lab for Neural Computation and Adaptation, RIKEN Center for Brain Science, Saitama, Japan

3, Department of Mathematical Informatics, Graduate School of Information Science and Technology, University of Tokyo, Tokyo, Japan

al., (2012)). Lubenov et al., (2009) suggests that these traveling waves spread along with anatomical structure rather than spatial distance.

The role of traveling waves is still unclear. One hypothesis is that the traveling waves mediate lateral propagation of signal within the cortex (Bringuier et al. (1999); Nauhaus et al., (2009)). Rubino et al. (2006) suggest that the waves mediate information transfer to distant neurons in movement preparation and execution. Another hypothesis is that slow oscillations during sleep contributes to memory consolidation (Rasch et al., (2007); Miyamoto et al., (2017)). Notably, while these works suggest the significance of traveling waves for learning, specific mechanisms are yet to be uncovered. We conducted computer simulations of neural network models to study this.

To explore the mechanism of how traveling waves contribute to learning, we model synaptic plasticity. Synaptic weight between a pair of neurons changes according to pre- and postsynaptic neural activity and a reward signal (Calabresi et al., (2007); Frémaux & Gerstner, (2016); Kuśmierz et al., (2017)). Reward-modulated spike-timing-dependent plasticity strengthens synapses that are contributing to eliciting a spike in the presence of a reward signal (Izhikevich, (2007); Klampfl & Maass, (2008)). While this learning rule tends to increase the probability of reproducing a spike sequence that leads to a reward, it cannot efficiently associate spiking activity among indirectly connected neurons. Signal transmission between indirectly connected neurons is crucial for task performance (Orsborn & Pesaran, (2017)) because most of the neurons in the brain are connected indirectly (Bassett & Bullmore, (2016)).

We hypothesized that a critical role of traveling waves is to propagate neural activity in between distant indirectly connected neurons. Consistently, Lubenov et al. (2009) mention that theta waves in rats' hippocampus assist signal transmission across areas such as to amygdala, hypothalamus, and medial prefrontal cortex, and this is also suggested in humans (Zhang et al., (2018); Zhang & Jacobs, (2015)). Traveling waves could gradually create a repertoire of paths spreading from a wave-initiating site. Once such repertoire is prepared, neurons are coherently activated along the paths so that reward-modulated STDP could select a subset of these paths to perform a task. We simulate computational models of reward-modulated STDP to study if traveling waves enhance learning.

## **2, Results**

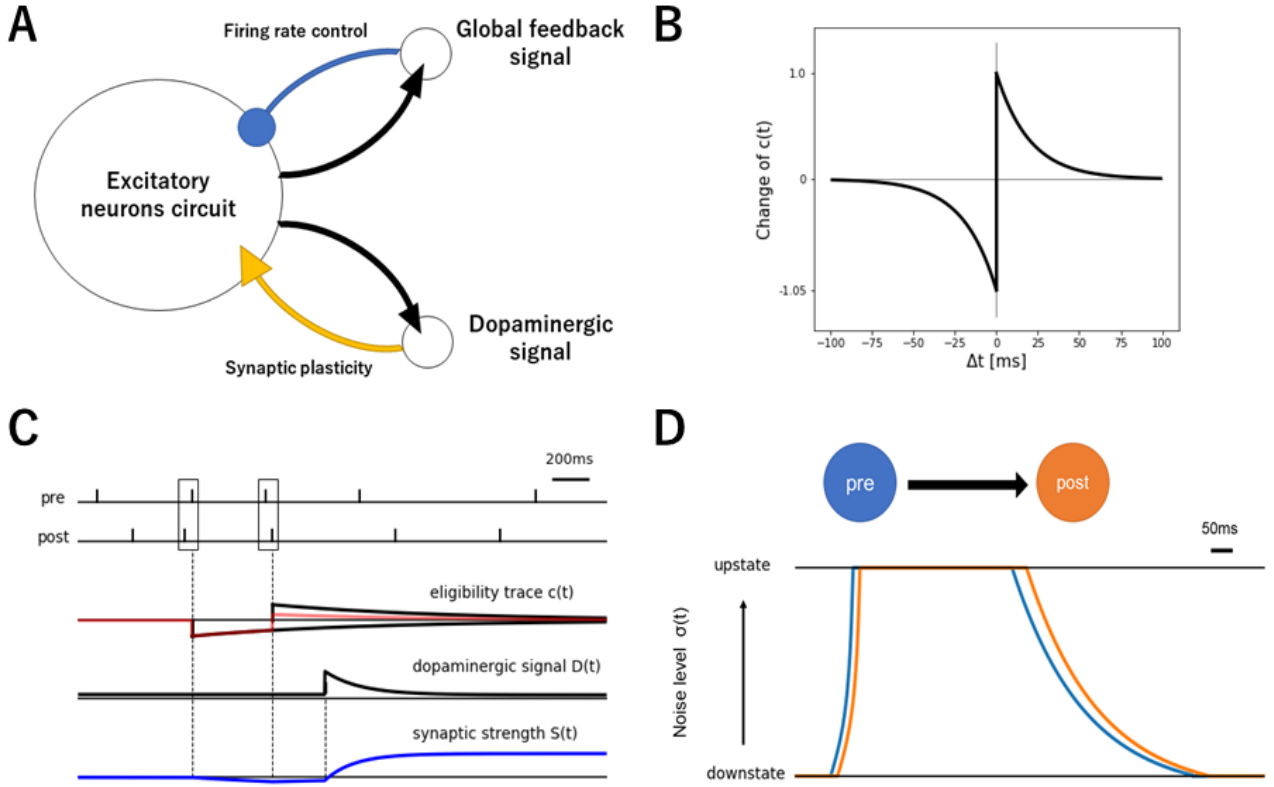


**Figure 1** Schematic explanation of the modified reward-modulated STDP rule. **A**, The whole network overview. **B**, The STDP learning window. **C**, The mechanism of synaptic plasticity. Synaptic weight changes as a product of eligible trace  $c(t)$  and dopaminergic signal  $D(t)$ . **D**, The upstate propagation from a presynaptic neuron to a postsynaptic neuron.

To demonstrate our hypothesis, we used relatively small excitatory spiking neural networks ( $N \sim 100$ ) with a global inhibitory signal and a global dopaminergic signal. Figure 1A explains the scheme of our setting. For the spiking neuron model, we adopted the leaky integrate-and-fire neuron. Dynamics of membrane potential  $v_i$  of neuron  $i$  are described by

$$dv_i/dt = [v_0 - v_i + h_i + h_i^{\text{ext}} - h]/\tau + \sigma_i(t)\xi_i$$

where  $v_0 = -74$  mV is resting potential,  $h_i$  is synaptic input from surrounding excitatory neurons,  $h_i^{\text{ext}}$  is external input to neuron  $i$ ,  $h$  is a global feedback signal that controls the overall firing rate of the network (see Methods for the expression), and  $\tau = 10$  ms is the membrane time constant.  $h_i$  is updated according to  $dh_i/dt = -h_i/\tau_o + \sum_j S_{ij} f_j(t - t_d)$ , with synaptic time constant  $\tau_o = 5$  ms, excitatory synaptic weight  $S_{ij}$  from neuron  $j$  to neuron  $i$ , spike train  $f_j$  of neuron  $j$  as a sum of delta functions peaking at neuron  $j$ 's spike timing, and synaptic transmission delay  $t_d = 2$  ms. The neuron emits a spike when  $v_i$  reaches a spiking threshold of  $-54$  mV and, then, is reset to resting potential

at  $-60$  mV. In addition, each neuron receives uncorrelated white Gaussian noise  $\xi_i$ . The noise level is controlled by a time-dependent standard deviation  $\sigma_i(t)$ , which is modulated by traveling waves as described below. A subset of neurons (stimulated neurons) receives external input as  $h_i^{\text{ext}}$  and other neurons receive no external input,  $h_i^{\text{ext}} = 0$  mV. The stimulated neurons receive input pulses at 500 Hz as  $h_i^{\text{ext}}$  that enforce them to spike during the first  $\sim 100$  ms of each learning trial (see below for each task setup).

As a synaptic plasticity rule (Figure 1B, C), we used a modified version of reward-modulated STDP. In the conventional model (Izhikevich (2007)), the dopaminergic signal is explained by one variable. However, recent research suggests that the dopaminergic signal has two different timescales: tonic and phasic component (Floresco et al., 2003). Therefore, we prepared corresponding tonic variable  $D_t$  and phasic variable  $D_p$  to describe these components. Specifically,  $D_t$  corresponds to the baseline dopamine level, while  $D_p$  represents the dopaminergic signal driven by a reward or punishment signal. Both of these dopaminergic components are assumed to be modulated by the novelty (Li et al., (2003)) of the task. Toward the end of simulations, both  $D_t$  and  $D_p$  declines once task performance improves (see Methods). Note that dopaminergic signals  $D_t$  and  $D_p$  are global variables common to all synapses. The synaptic weight  $S_{ij}$  ( $0 \leq S_{ij} \leq S_{\text{max}}$ ) from neuron  $j$  to  $i$  is adjusted according to

$$dS_{ij}/dt = c_{ij}(D_t + D_p)/\tau_s$$

where  $S_{\text{max}}$  is a task-dependent maximum synaptic weight (see Methods),  $\tau_s = 1$  ms is the timescale of the change, and  $c_{ij}$  ( $-S_{\text{max}}/2 \leq c_{ij} \leq S_{\text{max}}/2$ ) is so-called the STDP eligibility trace (Izhikevich (2007)) that accumulates the effects of plasticity events with time-constant  $\tau_c = 1000$  ms.

$$dc_{ij}/dt = -c_{ij}/\tau_c + \gamma \cdot (f_i \bar{f}_j - 1.05 \cdot \bar{f}_i f_j)$$

where  $f_i$  is the spike-train of neuron  $i$  and  $\bar{f}_i$  is the running average of  $f_i$  with time constant  $\tau_{\text{STDP}}$ . Here, STDP follows typical asymmetric window (Bi & Poo, (1998)) with task-dependent amplitude  $\gamma$  (see Methods) and fixed time-constant  $\tau_{\text{STDP}} = 20$  ms (Figure 1B). The upper- and lower-bounds of  $c_{ij}$  limits the speed of synaptic change.

Regarding the wave, we used a simple custom-made propagation rule. The upstate is defined as a high noise level state ( $\sigma_i(t) \sim 5.5$  mV), while the downstate is a low noise phase ( $\sigma_i(t) \sim 2$  mV). These noise levels roughly reproduce experimentally observed firing rate of 5 Hz in the upstate and 0 Hz in the downstate, respectively (Harris et al., 2010). The initial upstate spreads from externally stimulated neurons at each trial. Then, the upstate propagates from these neurons to peripheral neurons. The noise level is determined by  $\sigma_i(t) = \alpha_i \cdot \psi_i + 2$  mV with influx coefficient  $\alpha_i$  and local field  $\psi_i$ ,

representing the average activity of non-modeled neurons around neuron  $i$ . In order to control the noise level, we constrain the range of  $\sigma_i(t)$  between 2 mV to 5.5 mV and the range of  $\psi_i$  between -1 mV to 100 mV.  $\psi_i$  is updated (Figure 1D) by

$$d\psi_i/dt = (g_i(t) - \psi_i)/\tau_w + \left( \frac{0.2}{\delta t} \sum_{j \rightarrow i} [\psi_j(t - \delta t) - \psi_i(t) - \theta]_+ - \frac{0.1}{\delta t} \sum_{j \leftarrow i} [\psi_i(t - \delta t) - \psi_j(t) - \theta]_+ \right)$$

where  $\tau_w = 200$  ms is the time-constant of waves,  $\delta t = 15$  ms is a propagation delay,  $\theta = 0.001$  is a threshold for wave propagation, the expressions  $j \rightarrow i$  and  $j \leftarrow i$  respectively represent the sets of  $j$ 's that have connections incoming to and outgoing from neuron  $i$ .  $[x]_+$  is the rectified linear function that takes  $x$  for positive  $x$  and 0 otherwise.  $g_i(t)$  describes time-dependent drive for the local field  $\psi_i$  by external input. For stimulated neurons,  $g_i(t) = \eta \int_{t_{\text{on}}}^t h_i^{\text{ext}}(t') dt'$  integrates the external input from stimulation-onset time  $t_{\text{on}}$  while time  $t$  is in a simulation interval, and  $g_i(t) = -5$  mV after the stimulation interval. For non-stimulated neurons,  $g_i(t) = 0$  always holds. The gain factor  $\eta$  takes task-dependent value as described in Methods. Altogether, the local field around stimulated neurons rapidly increases at the beginning of each learning trial and, then, this activity diffuses as a wave to the local field of connected neurons. By the end of the learning trial of duration 2.5 s,  $\psi_i$  for all neurons decay close to zero. Neurons are placed on a two-dimensional square sheet. A rigid boundary condition is used so that waves collapse at the edges of the sheet.

Below, we conducted three tasks to illustrate our points.

### **Task 1: Selectively reinforcing distant paths**

Firstly, we demonstrate that the combination of traveling waves and STDP rule can strengthen a specific path from a stimulated neuron to a target neuron. This task is especially important in large-scale networks like the brains because most neurons are indirectly connected. A local STDP rule only does not efficiently solve this task because coherent activation of distant neurons is rare before learning. Wave signals compensate for this deficiency and facilitate learning of distant paths. This effect turns out to be evident, especially in the presence of tonic dopaminergic signal  $D_t$  which is not included in the conventional reward-modulated STDP rule. The  $D_t$  signal induces reward-independent STDP that synergistically work with traveling waves to prepare a repertoire of paths starting from the stimulated neuron (see below).

Figure 2 shows the setting and the result of this task. Figure 2A Left shows the initial network setting of this task. The central neuron in the grid (600  $\mu\text{m}$ , 600  $\mu\text{m}$ ) is stimulated by external input. The goal of this task is to strengthen the path from this stimulated neuron to the target neuron

positions at the bottom: (600  $\mu\text{m}$ , 100  $\mu\text{m}$ ). We also prepared three false-target neurons at the left: (100  $\mu\text{m}$ , 600  $\mu\text{m}$ ), right: (1100  $\mu\text{m}$ , 600  $\mu\text{m}$ ), and top: (600  $\mu\text{m}$ , 1100  $\mu\text{m}$ ), respectively. The central neuron is stimulated during the first 140 ms of each trial. This causes a traveling wave to build up there and spread to surrounding neurons gradually. If the target neuron spikes more than the other three false-target neurons during and after the stimulation, the reward signal  $D_p (> 0)$  is provided to the whole network. On the other hand, if any of the false-target neuron spikes more than the target neuron, the punishment signal  $D_p (< 0)$  is provided. We repeat trials of duration 2.5 s for 80 times in each simulation.

In a successful case, the paths from the stimulated neuron at the center to the target neuron at the bottom are selectively strengthened (Figure 2A). Figure 2B shows a successful example of firing rate of the target (red) and the false-target neurons' (black). The firing rate of the target neuron is selectively increased. The success rate of each condition is indicated in Figure 2C. The combination of traveling waves and  $D_t$  signal improves task performance compared with the conventional model of Izhikevich (2007).

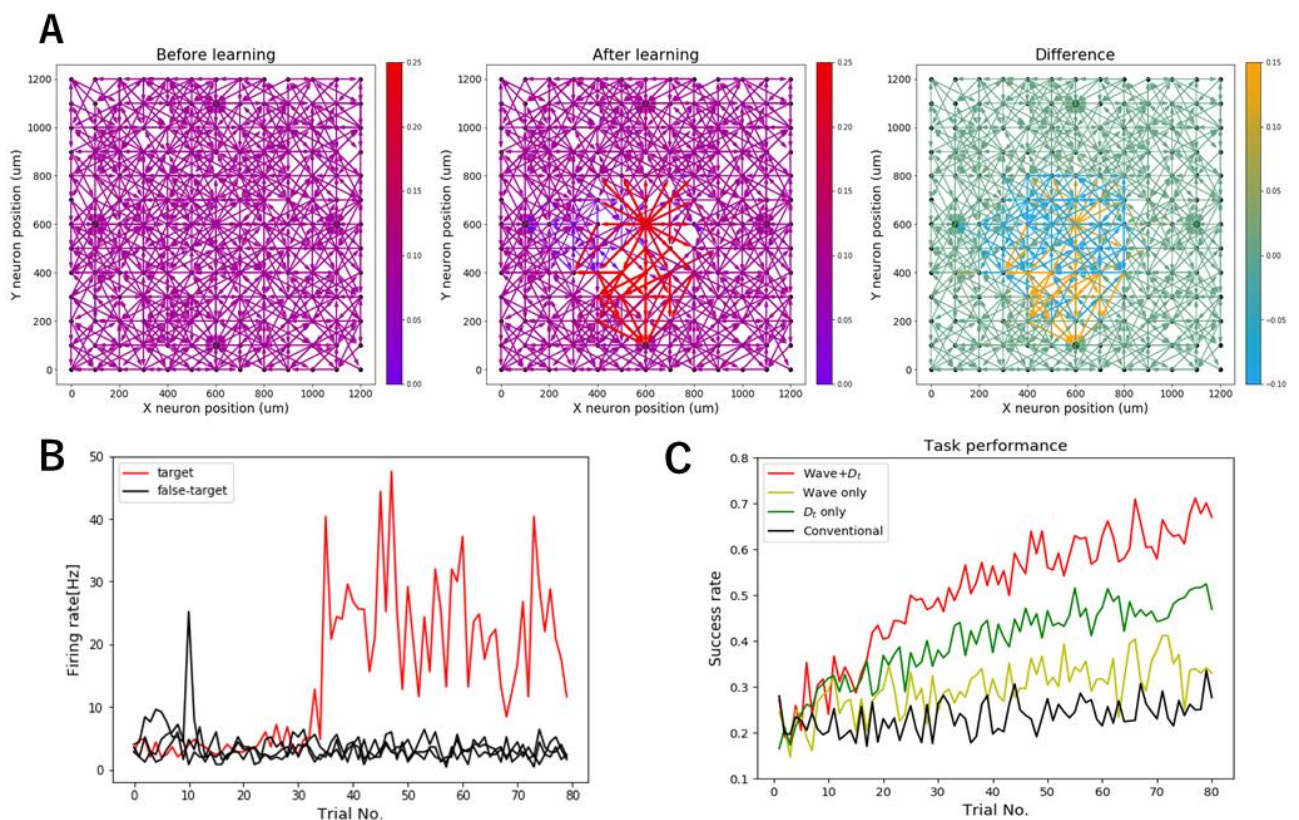


**Figure 2** Upstate propagation improves the reinforcement task of distant paths. **A**, An example of a successful trial. The initial synaptic weights are represented by color (Left). The path from a stimulated neuron (600  $\mu\text{m}$ , 600  $\mu\text{m}$ ) to a target neuron (600  $\mu\text{m}$ , 100  $\mu\text{m}$ ) is selectively strengthened at the end of the learning (Middle). The difference between the initial synaptic weights and the final synaptic

weights (Right). **B**, A successful example of this task. The firing rate of the target neuron selectively increases. **C**, The success rate of each condition (50 simulations averaged). A combination of wave and  $D_t$  signal (red line) shows the best task performance, while the conventional model (black line) fails to complete this task.

## Task 2: Finding a shortcut

The combination of wave signal and STDP rule can also be used to find the shortest paths from stimulated neuron to a target. Generally, finding short paths is vital for fast and reliable computation because information transmission through detour paths is slow and also fragile because successful transmission depends on multiple neurons' states, which are unreliable in nature. Finding a shortcut might be difficult without traveling waves because the neurons along the shortcut path would be seldom activated coherently. The wave propagation can significantly increase this probability and accelerate the exploring process.

Figure 3 shows the setting and the result of this task. Similar to Task 1, we devised a stimulated neuron and a target neuron. The stimulated neuron is located upper-left at (100  $\mu\text{m}$ , 500  $\mu\text{m}$ ), and the target neuron is located bottom-left at (100  $\mu\text{m}$ , 100  $\mu\text{m}$ ) (Figure 3A). The synaptic weights of detour paths ( $> 6$  path-length) are initially set twice as strong as the other synapses. The stimulated neuron receives external input at the beginning of each trial for 100 ms. Initially, the signal is only transferred through the detour path, which takes more than 100 ms to reach the target neuron. On the other hand, it takes less than 60 ms when the signal is transferred through the shortcut paths after learning.

In a successful case, shorter paths are strengthened while the detour paths are preserved (Figure 3A). Figure 3B shows the overall performance of this task. The wave condition with tonic dopaminergic signal  $D_t$  outperforms the conventional model. Figure 3C represents the averaged latency for obtaining reward after the trial onset in successful cases. The latency decreases faster than the other conditions with waves and the tonic dopaminergic signal. This result shows that our model successfully reaches the optimum solution by finding a shortcut.

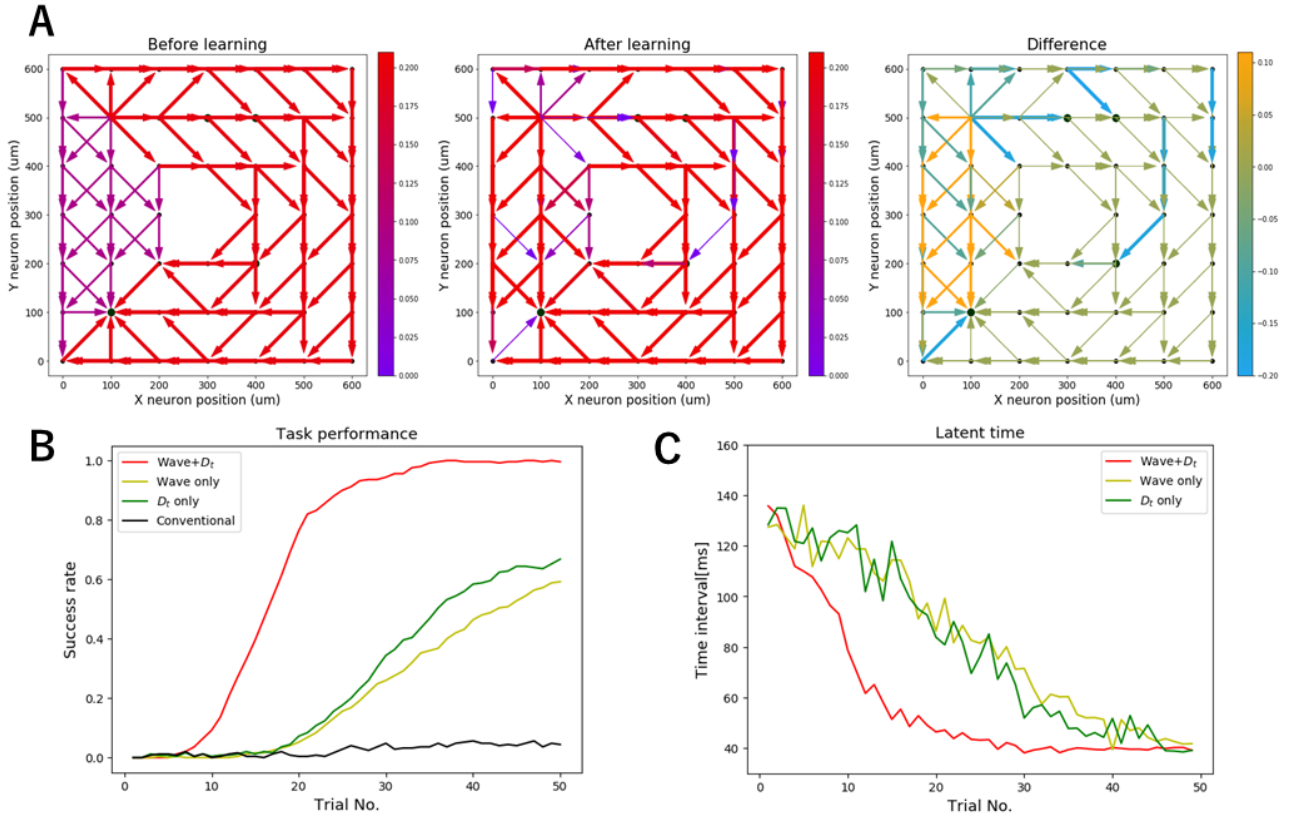


**Figure 3** Wave propagation helps to find a shortcut. **A**, A successful example of this task. Each panel represents the initial synaptic weight (Left), the last synaptic weight (Middle), and the difference between them (Right). The shorter path from the stimulated neuron on the upper-left at (100  $\mu\text{m}$ , 500  $\mu\text{m}$ ) to the target neuron on the bottom-left at (100  $\mu\text{m}$ , 100  $\mu\text{m}$ ) is strengthened while the detour paths between them are preserved. **B**, The success rate of each condition is plotted. The condition with waves and tonic dopaminergic signal  $D_t$  (red) shows the best performance, while the conventional model (black) fails. **C**, The latency of signal transmission from the stimulated neuron to the target neuron, averaged over successful simulations. (There is no success using the conventional model.)

### Task 3: Learning a nonlinear function (XOR)

In this task, we demonstrate that our model is useful for a more practical setting. Here, we show that XOR function can be learned in our model as well. Nonlinear functions like XOR function are essential for complex calculation, but how to realize them efficiently with reward-modulated STDP rule remains to be seen. We propose that our model has an advantage in this task because some nonlinear functions can be created by finding appropriate poly-synaptic paths. Among the various kinds of nonlinear functions, we chose XOR function because of its simplicity and the universality of



logic gates (Yang et al., (2011)). It is widely known that implementing XOR function requires a hidden layer in a feed-forward neural network. Therefore, this task is hard for STDP rule because indirect paths have to be learned. Our model can alleviate the difficulty and facilitate the learning process.

Figure 4 shows the setting and the result of this experiment. In this task, we used four stimulated neurons located at the bottom, namely, A (100  $\mu\text{m}$ , 0  $\mu\text{m}$ ), B (200  $\mu\text{m}$ , 0  $\mu\text{m}$ ), C (300  $\mu\text{m}$ , 0  $\mu\text{m}$ ), and D (400  $\mu\text{m}$ , 0  $\mu\text{m}$ ) (Figure 4A). In the middle line at  $Y = 100 \mu\text{m}$ , 500 neurons are aligned, and the stimulated neurons randomly project to the middle-layer neurons at a probability of 0.2. Two target neurons position at the top, namely, P (150  $\mu\text{m}$ , 200  $\mu\text{m}$ ) and Q (350  $\mu\text{m}$ , 200  $\mu\text{m}$ ), and each middle layer neuron connects to both of them. During this task, four different stimuli are provided, where one of the pairs of stimulated neurons AB, AC, BD, or CD receives external input. At the beginning of each trial, corresponding neurons are stimulated for 100ms. The target neuron for each of the four stimuli is P, Q, Q, and P, respectively. If the corresponding target neuron fires more than the other neuron, the reward signal  $D_p (> 0)$  is provide. Otherwise, the punishment signal  $D_p (< 0)$  is provided.

Figure 4A shows the synaptic weight change in successful case. The relevant connections are selectively strengthened or weakened. Figure 4B shows task performance of each condition. The wave conditions (red and yellow) performs better than the non-wave conditions (green and black). In the wave conditions, the performance is enhanced by learning synaptic weights between the stimulated and middle-layer neurons.

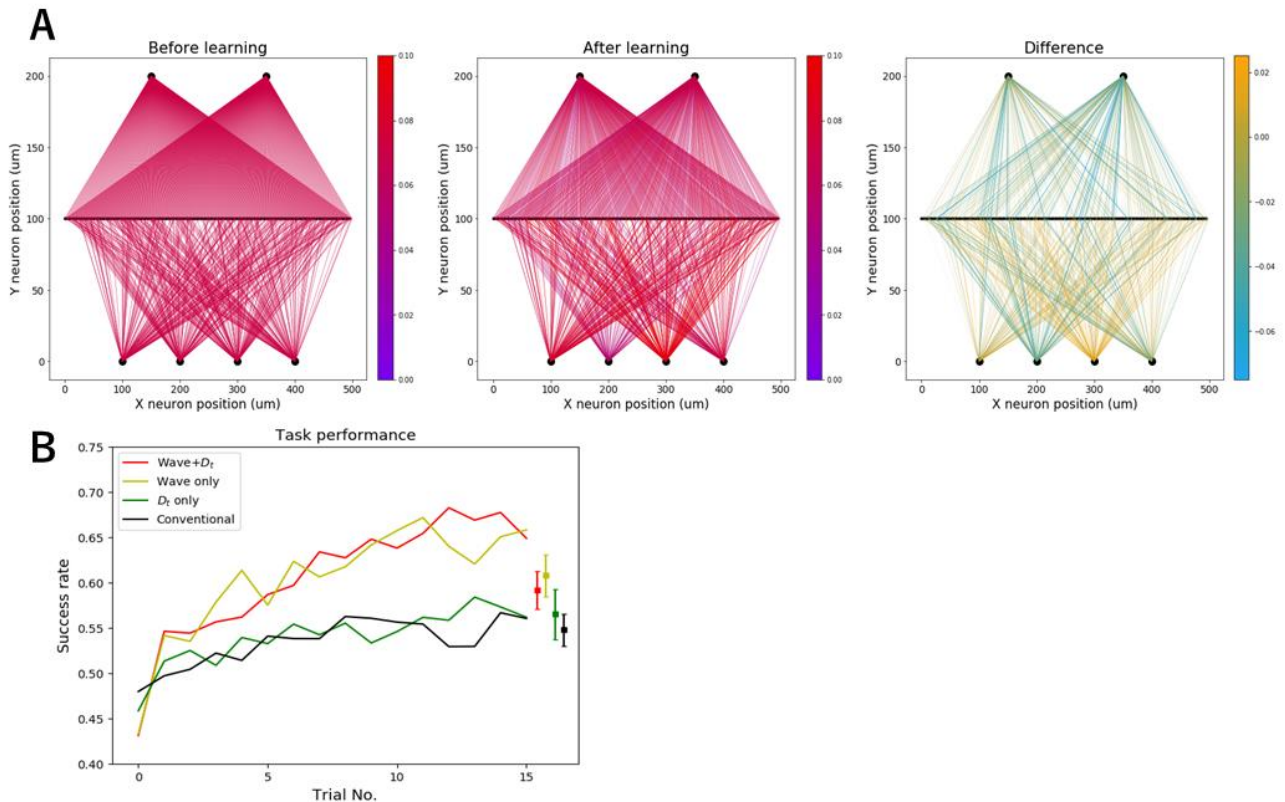


**Figure 4** Wave propagation is useful for learning a nonlinear function. **A**, A successful example of synaptic weight change. The Initial condition (Left), the last condition (Middle), and the difference (Right). **B**, The successful rate of XOR task. Wave conditions (red & yellow) shows better results than non-wave conditions (green & black). Squares show the success rate of the corresponding conditions when synaptic weights between stimulated and middle-layer neurons are reverted to their initial values. The error bar indicates the standard error of the mean.

### 3, Discussion

We have demonstrated that the combination of traveling waves and tonic dopaminergic signals enhances selective reinforcement of poly-synaptic paths. Further, we showed that this combination is also helpful for learning a nonlinear function. The advantage of traveling waves to send signals across distant neurons is effectively utilized in the tasks we explored. Thus, we argue that a possible role of traveling waves in the brain is to aid local learning rules, such as the reward-modulated STDP, to efficiently learn distant paths by inducing coherent activity in neurons along with them.

The advantage of the proposed model over the conventional model is twofold – First, the combination of traveling waves and the tonic dopaminergic signal helps to prepare paths starting from stimulated neurons. In our model, a tonic dopaminergic signal permits reward-independent STDP. In its presence, traveling waves efficiently create a repertoire of poly-synaptic paths spreading from the wave-initiation sites. Second, once a repertoire of paths from the stimulated neurons is prepared, then, a reward-dependent phasic dopaminergic signal can reinforce its subset. These features are consistent with biological evidence of recent studies. Beeler et al. (2010) showed that tonic and phasic dopamine have different roles: Tonic dopamine modulates the degree of learning and its expression, while phasic dopamine is the main source of reinforcement learning. Also, Schultz (2007) suggests that the continuous emission of tonic dopaminergic signals controls the motivation for exploration, while the discrete phasic dopaminergic signal induces the event-related synaptic plasticity. Our model is also testable by examining the relationship between traveling waves and learning under the specific environment such as selectively blockage or enhancement of either the tonic or phasic component of the dopaminergic signal.

Our model suggests a mechanism of memory consolidation during slow-wave sleep. Some experiments observed traveling waves across the entire brain during slow-wave sleep (Massimini et al., (2004); Mohajerani et al., (2010)) and showed their importance in memory consolidation (Miyamoto et al., (2017); Rasch et al. (2007)). Importantly, dopaminergic neurons emit tonic signals during slow wave sleep (Monti & Monti, (2007)). These works indicate that the combination of traveling

waves and tonic dopaminergic signals may consolidate memories. Our results agree with this view supporting that the coherent activation of neurons caused by traveling waves can prepare distant paths for more rapid and reliable signal transmission (c.f. Figure 3). Studies on the role of traveling waves and dopaminergic signals on poly-synaptic paths during slow-wave sleep likely elucidate the mechanism for memory consolidation.

One limitation of our model is the separation of dynamics between neural activities and wave propagation. In our model, wave propagation is modeled by the local field without specific relation to the membrane potential of neurons. While this approach is reasonable in our study that involves only a small number of neurons, the local field must be defined by the average activity level of many neurons in reality (Muller et al., 2018). Thus, future large-scale simulations could model the relation between traveling waves and the membrane potential of neurons in a more realistic manner. Further, the current model only involves global inhibition, but different classes of inhibitory neurons contribute to up- and down-states in distinct ways (Tahvildari et al., (2012)). More subtle features of traveling waves might arise from such detailed modeling. Despite these limitations, our simple model revealed a synergy of traveling waves and dopaminergic signals to efficiently learn the directionality of information flow and distant neural-network paths in a reinforcement task. This mechanism would be progressively more important for animals with a larger brain because distant and indirect paths are more dominant. Our study underscores the importance of coherent neural activity in the form of waves for coherent learning beyond pairs of neurons.

## 4, Methods

### Simulation environment

We conducted all the simulation with Brian2 simulator(<https://brian2.readthedocs.io/en/stable/>). This is an open python library that focuses on spiking neurons' simulation (Stimberg et al., 2019). The post analysis of the simulation is performed by custom made python code.

### Networks

The network of excitatory neurons is defined task by task (See Figure 2A, 3A, 4A). As described in Results, all excitatory neurons receive a global feedback signal and a dopaminergic signal in common for simplicity (Figure 1A).

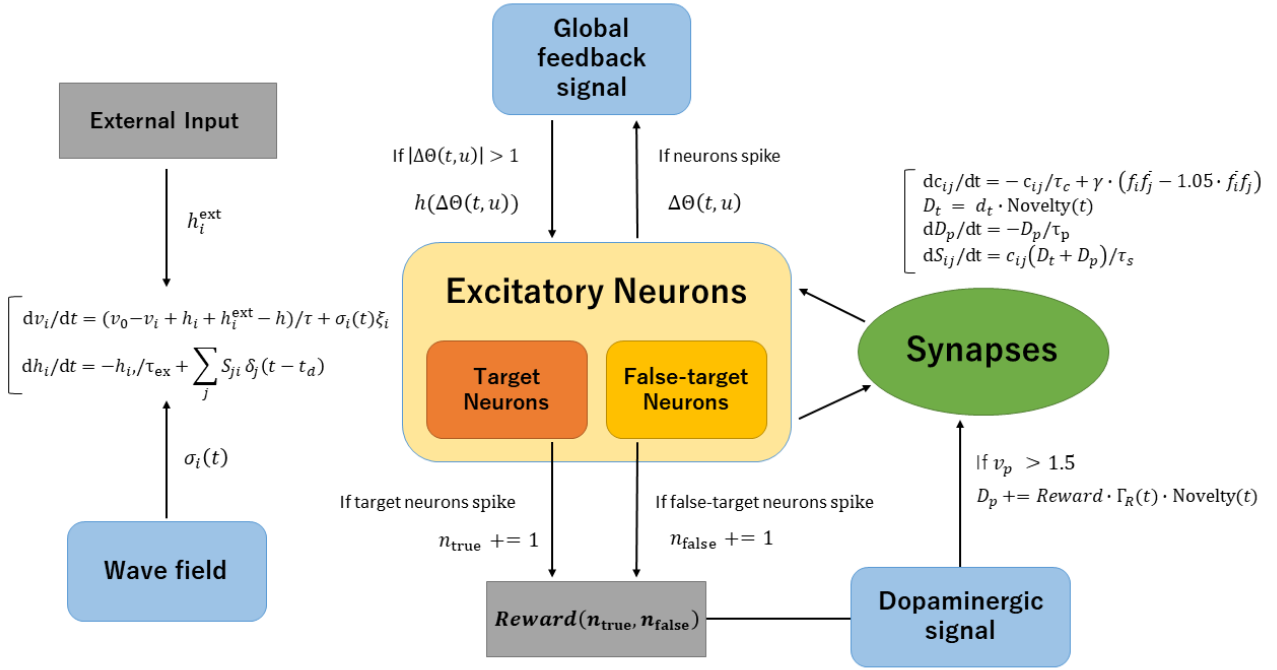


**Figure 5** The whole system of our model. Excitatory neurons are locally connected via synapses. Global feedback signal controls the firing rate of excitatory neurons, global dopaminergic signal modulates the synaptic weights, and wave field created by the activities of other neurons controls the activity level of each excitatory neuron. External input and reward function are externally provided.

### Global feedback signal

The global feedback signal  $h$  controls the firing rate of excitatory neurons. This variable depends on interval-weighted activity  $\Theta_i(t) = \int_u^t (s-u)f_i(s)ds$  of neuron  $i$ , where  $u$  indicates the latest time the global feedback signal is transmitted, and  $\Theta^* = 1$ . The difference  $\Delta\theta(t)$  is described by

$$\Delta\theta(t) = \sum_i \Theta_i(t) - (t-u)\Theta^*$$

When the firing-rate difference reaches  $\Delta\theta < -1$  at time  $s$ , a global feedback input of  $h(t) = \beta_1 \Delta\theta(s) \delta(t-s-t_h)$  mV with Dirac's delta function  $\delta$  is transmitted after transmission delay  $t_h = 1$  ms. On the other hand, when firing-rate difference reaches  $\Delta\theta > 1$  at time  $s$ , a global feedback input of  $h(t) = \beta_2 \Delta\theta(s)^2 \delta(t-s-t_h)$  mV is transmitted. This inhibition is  $\propto \Delta\theta^2$  to prevent runaway neural activity due to the excitatory recurrent input. The values of  $\beta_1$  and  $\beta_2$ , summarized in Table 1, depend on each task because of the difference in the number of neurons and the network structure.

## Dopaminergic signal

The tonic dopaminergic signal  $D_t$  and the phasic dopaminergic signal  $D_p$  are essential ingredients of our simulations.  $D_t$  signal is expressed by

$$D_t = d_t \cdot \text{Novelty}(t)$$

with tonic dopamine constant  $d_t$ , and the novelty function  $\text{Novelty}(t)$  (explained below). We used task-dependent values for  $d_t$  as summarized in Table 1. The network in Task 1 requires relatively larger baseline synaptic fluctuation compared to Task 2 and 3.

$D_p$  signal ( $-0.3 \leq D_p \leq 0.3$ ) is adjusted depending on the performance of each task.  $D_p$  depends on three variables: reward  $R$ , decay-function  $\Gamma_R$  for the reward, and novelty variable  $\text{Novelty}$  (Figure 5). We measured the spike counts of target and false-target neurons by vectors  $n_{\text{true}}$  and  $n_{\text{false}}$ , respectively, in each trial. (These vectors are reset to zero at the end of each trial.) Reward  $R$  is a function of  $n_{\text{true}}$  and  $n_{\text{false}}$ . For Task 1,  $R = 0$  when the total spike-count of the one target and three false-target neurons is less than 5. This adds robustness to the simulation result. Once the total spike-count reaches 5,  $R = 1.0$  when the target spike-count is the greatest and  $R = -0.5$  when the target spike-count is not the greatest among the four neurons. Namely,

$$R = (-0.5 + 1.5 I[n_{\text{true}} > \max(n_{\text{false}})])(n_{\text{true}} + \text{sum}(n_{\text{false}}) > 5)$$

where  $I[\cdot]$  is the indicator function that takes 1 if the argument is true and takes 0 otherwise. We mean by  $\max(n_{\text{false}})$  and  $\text{sum}(n_{\text{false}})$  the maximum and the sum of the spike counts of the three false-target neurons, respectively.

For Task 2, there are one target neuron and no false-target neuron. Therefore, we used

$$R = I[n_{\text{true}} > 5]$$

In this task, punishment ( $R < 0$ ) is not given.

For Task 3, we again consider one target neuron and one false-target neuron.  $R = 1$  when the target neuron fires at least more than five spikes than the false target neuron;  $R = -1$  when the false-target neuron fires at least more than five spikes than the target neuron; and  $R = 0$  otherwise. Namely,

$$R = (I[n_{\text{true}} \geq n_{\text{false}} + 5] - I[n_{\text{false}} \geq n_{\text{true}} + 5])$$

We set this margin of five spikes to induce a clear difference in the number of spikes between the target and false-target neurons.

Next, we introduce reward-decay function  $\Gamma_R$ . The amount of reward begins to take a non-zero value after the stimulus onset time  $t_{on}$ , stay fixed until the stimulus offset time  $t_{off}$ , and then decays exponentially. Namely,

$$\Gamma_R(t) = d_p I[t > t_{on}] e^{-\frac{t-t_{off}}{\tau_d}}$$

with dopamine decay constant  $\tau_d = 200$  ms and the initial amplitude  $d_p$ , which is set depending on the tasks (see Table 1).

Finally, we assume that dopamine releases increase with novelty (Feenstra et al., (1995)) and novelty becomes high when prediction error is high. We simply assume that Novelty ( $0 \leq \text{Novelty} \leq 1$ ) decreases by 0.2 at the end of a correct trial and increases by 0.2 at the end of a wrong trial within the permitted range. Here, we introduce task-dependent correct and incorrect criteria. In Task 1 and 3, we used  $R > 0$  and  $R \leq 0$  at the end of each trial to define a correct and incorrect trial, respectively. In Task 2, we used the latency of signal transmission from the stimulated neuron to the target neuron for the criteria. A latency less than 60 ms is defined correct, and is otherwise wrong.

In our model, the target or false-target neurons occasionally spikes due to noise. In order to suppress phasic dopamine release in response to a noise-induced spike, we introduce a variable  $v_p$ . This value increases by 1 every time a target neuron or a false-target neuron spike, and decays according to

$$dv_p/dt = -v_p/\tau_p$$

with time-constant  $\tau_p = 10$  ms. When  $v_p$  reaches 1.5,  $D_p$  is incremented with transmission delay of 100 ms by the product  $R \cdot \Gamma_R \cdot \text{Novelty}$ , and then  $v_p$  is reset to zero. This condition roughly means that a phasic dopaminergic signal is emitted if a target neuron or false-target neurons emit two spikes within 7 ms. This rarely happens due to noise.

## Influx coefficient

Regarding the wave, we used a simple custom-made propagation rule. The upstate is defined as a high noise level state ( $\sigma_i(t) \sim 5.5$  mV), while the downstate is a low noise phase ( $\sigma_i(t) \sim 2$  mV). The noise level is determined by  $\sigma_i(t) = \alpha_i \cdot \psi_i + 2$  mV with influx coefficient  $\alpha_i$  and local field  $\psi_i$ . The local field is updated as explained in Results. The influx coefficient quantifies the sensitivity of neuron  $i$ 's noise level on  $\psi_i$  and is defined by

$$\alpha_i(t) = 5 \cdot \tanh \left( \int_{t_{on}}^t \sum_{j \rightarrow i} \delta(\psi_j(t - \delta t) - \psi_i(t) - \theta) dt \right)$$

where  $t_{\text{on}}$  is again the trial onset. The coefficient  $\alpha_i$  counts the number of local fields that influence  $\psi_i$  in each trial up to time  $t$ . Tangent hyperbolic function is introduced for normalization.

	Experiment 1	Experiment 2	Experiment 3
$N$	136	49	506
Network type	Recurrent	Feedforward	Feedforward
$\beta_1$ [mV]	1.2	1.5	1.0
$\beta_2$ [mV]	1.5	0.05	0.2
$S_{\text{max}}$	15	12.6	6.0
$\gamma$	0.3	0.3	0.06
$d_t$	5e-3	3e-3	3e-3
$d_p$	0.02	0.005	0.015
Target distance	3~5 neurons	2~4 neurons	2 neurons
$\eta$	5	5	1

**Table 1** The task-dependent variables are summarized.

## 5, References

W. Klimesch. 1996. Memory processes, brain oscillations and EEG synchronization. International Journal of Psychophysiology.

G.R. Burkitt, R.B. Silberstein & P.J. Cadusch, A.W. Wood. 2000. The steady-state visually evoked potential and travelling waves. Clinical Neurophysiology.

P.L. Nunez & R. Srinivasan. 2006. Electric fields of the brain: The neurophysics of EEG. Oxford University Press.

R. Srinivasan, F.A. Bibi & P.L. Nunez. 2006. Steady-state visual evoked potentials: distributed local sources and wave-like dynamics are sensitive to flicker frequency. Brain Topography.

A. Grinvald, E.E. Lieke, Ron D. Frostig, & R. Hildesheim. 1994. Cortical point-spread function and long-range lateral interactions revealed by real-time optical imaging of macaque monkey primary visual cortex. Journal of Neuroscience.

- H. Slovin, A. Arieli, R. Hildesheim & A. Grinvald. 2002. Long-term voltage-sensitive dye imaging reveals cortical dynamics in behaving monkeys. *Journal of Neurophysiology*.
- I. Nauhaus, L. Busse, M. Carandini & D.L. Ringach. 2009. Stimulus contrast modulates functional connectivity in visual cortex. *Nature Neuroscience*.
- I. Nauhaus, L. Busse, D.L. Ringach & M. Carandini. 2012. Robustness of traveling waves in ongoing activity of visual cortex. *Journal of Neuroscience*.
- M.H. Mohajerani, D.A. McVea, M. Fingas & T.H. Murphy. 2010. Mirrored bilateral slow-wave cortical activity within local circuits revealed by fast bihemispheric voltage-sensitive dye imaging in anesthetized and awake mice. *Journal of Neuroscience*.
- M. Massimini, R. Huber, F. Ferrarelli, S. Hill & G. Tononi. 2004. The sleep slow oscillation as a traveling wave. *Journal of Neuroscience*.
- S. Sakata & K.D. Harris. 2009. Laminar structure of spontaneous and sensory-evoked population activity in auditory cortex. *Neuron*.
- K.D. Harris & Alexander Thiele. 2011. Cortical state and attention. *Nature Reviews Neuroscience*.
- C.C. Petersen, A. Grinvald & B. Sakmann. 2003. Spatiotemporal dynamics of sensory responses in layer 2/3 of rat barrel cortex measured in vivo by voltage-sensitive dye imaging combined with whole-cell voltage recordings and neuron reconstructions. *Journal of Neuroscience*.
- M Steriade, D.A. McCormick & T.J. Sejnowski. 1993. Thalamocortical oscillations in the sleeping and aroused brain. *Science*.
- E.M. Krull, S. Sakata & T. Toyoizumi. 2019. Theta oscillations alternate with high amplitude neocortical population within synchronized states. *Frontiers in Neuroscience*.
- B.R. Lee, P. Mu, D.B. Saal, C. Ulibarri & Yan Dong. 2008. Homeostatic recovery of downstate–upstate cycling in nucleus accumbens neurons. *Neuroscience Letters*.
- T.K. Sato, I. Nauhaus & M. Carandini. 2012. Traveling waves in visual cortex. *Neuron*.
- E.V. Lubenov & A.G. Siapas. 2009. Hippocampal theta oscillations are travelling waves. *Nature*.



- V. Bringuier, F. Chavane, L. Glaeser & Y. Frégnac. 1999. Horizontal propagation of visual activity in the synaptic integration field of area 17 neurons. *Science*.
- D. Rubino, K.A. Robbins & N.G. Hatsopoulos. 2006. Propagating waves mediate information transfer in the motor cortex. *Nature Neuroscience*.
- B. Rasch, C. Büchel, S. Gais & J. Born. 2007. Odor cues during slow-wave sleep prompt declarative memory consolidation. *Science*.
- D. Miyamoto, D. Hirai & M. Murayama. 2017. The roles of cortical slow waves in synaptic plasticity and memory consolidation. *Frontiers in Neural Circuits*.
- P. Calabresi, B. Picconi, A. Tozzi & M.D. Filippo. 2007. Dopamine-mediated regulation of corticostriatal synaptic plasticity. *Trends in Neuroscience*.
- N. Frémaux & W. Gerstner. 2016. Neuromodulated spike-timing-dependent plasticity, and theory of three-factor learning rules. *Frontiers in Neural Circuits*.
- Ł. Kuśmierz, T. Isomura & T. Toyoizumi. 2017. Learning with three factors: modulating Hebbian plasticity with errors. *Current Opinion in Neurobiology*.
- E.M. Izhikevich. 2007. Solving the distal reward problem through linkage of STDP and dopamine signaling. *Cerebral Cortex*.
- S. Klampfl & W. Maass. 2008. Emergence of dynamic memory traces in cortical microcircuit models through STDP. *Journal of Neuroscience*.
- A.L. Orsborn & B. Pesaran. 2017. Parsing learning in networks using brain–machine interfaces. *Current Opinion in Neurobiology*.
- D.S. Bassett & E.T. Bullmore. 2016. Small-world brain networks revisited. *The Neuroscientist*.
- H. Zhang, A.J. Watrous, A. Patel & J. Jacobs. 2018. Theta and alpha oscillations are traveling waves in the human neocortex. *Neuron*.
- H. Zhang & J. Jacobs. 2015. Traveling theta waves in the human hippocampus. *Journal of Neuroscience*.

- S.B. Floresco, A.R. West, B. Ash, H. Moore & A.A. Grace. 2003. Afferent modulation of dopamine neuron firing differentially regulates tonic and phasic dopamine transmission. *Nature Neuroscience*.
- S. Li, W.K. Cullen, R. Anwyl & M.J. Rowan. 2003. Dopamine-dependent facilitation of LTP induction in hippocampal CA1 by exposure to spatial novelty. *Nature Neuroscience*.
- G.Q. Bi & M.M. Poo. 1998. Synaptic modifications in cultured hippocampal neurons: dependence on spike timing, synaptic strength, and postsynaptic cell type. *Journal of neuroscience*.
- J. Yang, W. Yang & Wei Wu. 2011. A novel spiking perceptron that can solve XOR problem. *Neural Network World*.
- K.D. Harris, P. Bartho, P. Chadderton, C. Curto, J. Rocha, L. Hollender, V. Itskov, A. Luczak, S. L. Marguet, A. Renart & S. Sakata. 2010. How do neurons work together? Lessons from auditory cortex. *Hearing Research*.
- J.A. Beeler, N. Daw, Cristianne R.M. Frazier & X. Zhuang. 2010. Tonic dopamine modulates exploitation of reward learning. *Frontiers in Behavioral Neuroscience*.
- W. Schultz. 2007. Behavioral dopamine signals. *Trends in Neurosciences*.
- J.M. Monti, & D. Monti. 2007. The involvement of dopamine in the modulation of sleep and waking. *Sleep Medicine Reviews*.
- L. Muller, F. Chavane, J. Reynolds & T.J. Sejnowski. 2018. Cortical travelling waves: mechanisms and computational principles. *Nature Reviews Neuroscience*
- B. Tahvildari, M. Wolfel, A. Duque & D.A. McCormick. 2012. Selective functional interactions between excitatory and inhibitory cortical neurons and differential contribution to persistent activity of the slow oscillation. *Journal of Neuroscience*.
- M. Stimberg, R. Brette & D.F.M. Goodman. 2019. Brian 2: an intuitive and efficient neural simulator. *eLIFE*.
- M.G.P. Feenstra, M.H.A. Botterblom, J.F.M. van Uum. 1995. Novelty-induced increase in dopamine release in the rat prefrontal cortex in vivo: inhibition by diazepam. *Neuroscience Letters*.